arXiv:2107.08858v2 [cs.IT] 27 Sep 2021

Regular Perturbation and Achievable Rates of Space-Division Multiplexed Optical Channels

Francisco Javier García-Gómez and Gerhard Kramer

***Abstract*—Regular perturbation is applied to space-division multiplexing (SDM) on optical fibers and motivates a correlated rotation-and-additive noise (CRAN) model. For S spatial modes, or $2S$ complex-alphabet channels, the model has $4S(S+1)$ hidden independent real Gauss-Markov processes, of which $2S$ model phase noise, $2S(2S-1)$ model spatial mode rotation, and $4S$ model additive noise. Achievable information rates of multi-carrier communication are computed by using particle filters. For $S=2$ spatial modes with strong coupling and a 1000 km link, joint processing of the spatial modes gains 0.5 bits/s/Hz/channel in rate and 1.4 dB in power with respect to separate processing of $2S$ complex-alphabet channels without considering CRAN.**

***Index Terms*—Capacity, multi-mode, optical fiber, space-division multiplexing.**

I. Introduction

Space-division multiplexing (SDM) via multi-core and multi-mode transmission considerably increases the capacity of optical fibers [1]. Several experiments reaching 10 Pbit/s have been reported, e.g., see [2]–[4]. The analysis in [5], [6] generalizes to SDM and gives a spectral efficiency upper bound of $\log_2(1+\text{SNR})$ bits/s/Hz/channel, where SNR is the signal-to-noise ratio without the fiber nonlinearity and "channel" refers to a complex-alphabet channel.

Various mismatched models have been developed to compute achievable rates for single and dual polarization (1-pol, 2-pol) transmission [7]–[9]. We focus on models based on regular perturbation (RP) [10]–[13] and logarithmic perturbation (LP) [14], [15]. A combined RP and LP model is motivated in [16], see also [17], [18].

We follow [19], [20] and develop an analysis for SDM by using the coupling equations in [21], [22], RP, and an approximation related to LP. The result is a correlated rotation-and-additive noise (CRAN) model with correlated phase noise, spatial mode rotations, and additive noise. We use the model to compute achievable rates for SDM channels.

Notation: We use similar notation as in [19] and refer to that paper for details. For instance, we write the Fourier transform of a function $u(t)$ as $\mathcal{F}(u(t))$ and the inverse Fourier transform of $U(\Omega)$ as $\mathcal{F}^{-1}(U(\Omega)) = \mathcal{F}^{-1}(U(\Omega))(t)$. For vectors, operators such as $\mathcal{F}$ and $\mathcal{F}^{-1}$ are applied entrywise.

II. Space-Division Multiplexing

Each spatial mode has two complex-alphabet channels with the same spatial field distribution but orthogonal polarization. Consider S spatial modes, i.e., $2S$ complex-alphabet channels in total.[1] The propagating signal is

$$\mathbf{u}(z,t) = \left(\mathbf{u}^{[1]}(z,t)^T \quad \mathbf{u}^{[2]}(z,t)^T \quad \cdots \quad \mathbf{u}^{[S]}(z,t)^T\right)^T \quad (1)$$

where $\mathbf{u}^{[s]}(z,t) = (u^{[s]}(z,t), \overline{u}^{[s]}(z,t))^T$ is the vector of signals of the s-th spatial mode, $s=1,\ldots,S$. The variable z represents distance and t is time. We consider the following two propagation scenarios. The models assume that fiber birefringence changes randomly with z [21].

Weak Coupling: the linear coupling among spatial modes is neglected, which is reasonable for multi-core transmission. The propagation equation for spatial mode s is [21, Eq. (26)]

$$\frac{\partial \mathbf{u}^{[s]}}{\partial z} = j\beta_0^{[s]}\mathbf{u}^{[s]} - \beta_1^{[s]}\frac{\partial \mathbf{u}^{[s]}}{\partial t} - j\frac{\beta_2^{[s]}}{2}\frac{\partial^2 \mathbf{u}^{[s]}}{\partial t^2} + \frac{\mathbf{n}^{[s]}}{\sqrt{g_s(z)}} + j\gamma\left(f_{s,s}g_s(z)\left\|\mathbf{u}^{[s]}\right\|^2 + \sum_{r\neq s} f_{s,r}g_r(z)\left\|\mathbf{u}^{[r]}\right\|^2\right)\mathbf{u}^{[s]} \quad (2)$$

where $\beta_0^{[s]}$, $\beta_1^{[s]}$, and $\beta_2^{[s]}$ are the coefficients of the Taylor expansion of the propagation constant $\beta(\Omega)$ in the angular frequency Ω, averaged over the two polarizations. The noise signals $\mathbf{n}^{[s]} = (n^{[s]}(z,t), \overline{n}^{[s]}(z,t))^T$ are independent Wiener processes in z such that, in the absence of nonlinearity ($\gamma=0$), the accumulated noise in a bandwidth of $\mathcal{B}_{\text{ASE}}$ at $z=\mathcal{L}$ has autocorrelation function (ACF) $N_{\text{ASE}}\mathcal{B}_{\text{ASE}}\text{sinc}(\mathcal{B}_{\text{ASE}}(t-t'))$. The nonlinear coupling coefficients γ and $f_{s,s'}$ are described in [21]. Note that we have absorbed the factors $(8/9)$ and $(4/3)$ from [21, Eq. (26)] into $f_{s,s'}$. The functions $g_s(z)$ account for attenuation and amplification. Ideal distributed amplification (IDA) has $g_s(z)=1$.

Strong Coupling: the linear coupling between modes is strong, i.e., the vector $\mathbf{u}$ is subject to random unitary transformations that change rapidly with z. This has an averaging effect that simplifies (2) to [21, Eq. (38)]

$$\frac{\partial \mathbf{u}}{\partial z} = -j\frac{\beta_2}{2}\frac{\partial^2 \mathbf{u}}{\partial t^2} + j\gamma\kappa g(z)\left\|\mathbf{u}\right\|^2\mathbf{u} + \frac{\mathbf{n}}{\sqrt{g(z)}} \quad (3)$$

where $\mathbf{n}(z,t)$ has the same statistics as $(\mathbf{n}^{[1],T},\ldots,\mathbf{n}^{[S],T})^T$, the average dispersion coefficient is $\beta_2 = (\sum_s \beta_2^{[s]})/S$, and κ is defined in [21].

We develop a SDM-CRAN model for weak coupling. The model for strong coupling is a special case with the parameters $\beta_0^{[s]} = \beta_1^{[s]} = 0$, $\beta_2^{[s]} = \beta_2$ and $f_{s,s'} = \kappa$.

Date of current version September 28, 2021. This work was supported by the German Research Foundation (DFG) under Grants KR 3517/8-1 and 3517/8-2. (*Corresponding author: Francisco Javier García-Gómez.*)

The authors are with the Institute for Communications Engineering (LNT), Technical University of Munich, 80333 Munich, Germany (e-mail: javier.garcia@tum.de; gerhard.kramer@tum.de).

[1]This paper refers to mode-division multiplexing but equation (2) also applies to multi-core transmission under certain conditions [21].

Copyright (c) 2021 IEEE. Personal use is permitted. For any other purposes, permission must be obtained from the IEEE by emailing pubs-permissions@ieee.org.

III. Regular Perturbation

We expand $\mathbf{u}^{[s]}$ in (2) in powers of a small perturbation γ:

$$\mathbf{u}^{[s]}(z,t) = \mathbf{u}_0^{[s]}(z,t) + \gamma \Delta \mathbf{u}^{[s]}(z,t) + \mathcal{O}(\gamma^2). \quad (4)$$

The steps are the same as in [19], [20] and we arrive at

$$\mathbf{u}_0^{[s]}(z,t) = \mathbf{u}_{\text{LIN}}^{[s]}(z,t) + \mathbf{u}_{\text{ASE}}^{[s]}(z,t) \quad (5)$$

where $\mathbf{u}_{\text{LIN}}^{[s]}(z,t) = \mathcal{D}_z^{[s]} \mathbf{u}^{[s]}(0,t)$ and

$$\begin{aligned}
&\Delta \mathbf{u}^{[s]}(z,t) \\
&= j\mathcal{D}_z^{[s]} \left[\int_0^z \mathcal{D}_{-z'}^{[s]} \left(f_{s,s} g_s(z') \left\| \mathbf{u}_0^{[s]}(z',t) \right\|^2 \mathbf{u}_0^{[s]}(z',t) \right.\right. \\
&\left.\left. + \sum_{r \neq s} f_{s,r} g_r(z') \left\| \mathbf{u}_0^{[r]}(z',t) \right\|^2 \mathbf{u}_0^{[s]}(z',t) \right) \mathrm{d}z \right] \quad (6)
\end{aligned}$$

where

$$\mathcal{D}_z^{[s]} u(t) = \mathcal{F}^{-1} \left(e^{j\left(\beta_0^{[s]} - \beta_1^{[s]}\Omega + \frac{\beta_2^{[s]}}{2}\Omega^2\right) z} \mathcal{F}\left(u(t)\right) \right). \quad (7)$$

The effect of $\beta_0^{[s]}$ is a z-dependent phase shift, and the effect of $\beta_1^{[s]}$ is a z-dependent delay. Similar to [20], the $2S$ entries of the S noise signals $\mathbf{u}_{\text{ASE}}^{[s]}(z,t)$ are independent circularly-symmetric complex Gaussian (CSCG) processes. At the end of the fiber ($z = \mathcal{L}$), their ACF for $\gamma = 0$ is $N_{\text{ASE}}\, \mathcal{B}_{\text{ASE}}\, \text{sinc}(\mathcal{B}_{\text{ASE}}(t-t'))$.

We use pulse amplitude modulation (PAM) and wavelength division multiplexing (WDM). The indexes c of the WDM channels are in the set $\{c_{\min}, \cdots, 0, \cdots, c_{\max}\}$. The center angular frequency of channel c is Ω_c, and the WDM channel of interest (COI) has $c = 0$ and $\Omega_0 = 0$. The transmitted signal of spatial mode s is

$$\begin{aligned}
\mathbf{u}^{[s]}(0,t) = &\sum_{m=-\infty}^{\infty} \begin{pmatrix} x_m^{[s]} s(t - mT - \tau_0^{[s]}) \\ \overline{x}_m^{[s]} s(t - mT - \overline{\tau}_0^{[s]}) \end{pmatrix} \\
&+ \sum_{c \neq 0} e^{j\Omega_c t} \sum_{k=-\infty}^{\infty} \begin{pmatrix} b_{c,k}^{[s]} s(t - kT - \tau_c^{[s]}) \\ \overline{b}_{c,k}^{[s]} \overline{s}(t - kT - \overline{\tau}_c^{[s]}) \end{pmatrix} \quad (8)
\end{aligned}$$

where T is the symbol period. The base pulse $s(t)$ has most of its energy in the frequency band $|\Omega| \leq \pi\mathcal{B}$. The channels may have different delays $\tau_c^{[s]}$ and $\overline{\tau}_c^{[s]}$. The transmit symbols of the COI ($c = 0$) are $x_m^{[s]}$ and $\overline{x}_m^{[s]}$, and the transmit symbols of the interfering frequencies are $b_{c,k}^{[s]}$ and $\overline{b}_{c,k}^{[s]}$, $c \neq 0$. We consider symmetric symbol energies and fourth moments:

$$\begin{aligned}
E &= \left\langle |X_m^{[s]}|^2 \right\rangle = \left\langle |\overline{X}_m^{[s]}|^2 \right\rangle, && \text{all } s,\, m \\
E_c &= \left\langle |B_{c,k}^{[s]}|^2 \right\rangle = \left\langle |\overline{B}_{c,k}^{[s]}|^2 \right\rangle, && \text{all } s,\, k,\, c \neq 0 \\
Q_c &= \left\langle |B_{c,k}^{[s]}|^4 \right\rangle = \left\langle |\overline{B}_{c,k}^{[s]}|^4 \right\rangle, && \text{all } s,\, k,\, c \neq 0.
\end{aligned} \quad (9)$$

The receiver applies a band-pass filter $h_{\mathcal{B}}(t)$ followed by linear distortion compensation (LDC) or digital back-propagation (DBP), a matched filter, and a sampler:

$$y_m^{[s]} = \int_{-\infty}^{\infty} s_0^*(t - mT) \left\{ \mathcal{D}_{-\mathcal{L}}^{[s]} \left[h_{\mathcal{B}}(t) * u^{[s]}(\mathcal{L},t) \right] \right\} \mathrm{d}t. \quad (10)$$

We focus on $y_m^{[s]}$ to save space. Due to symmetry, the model for $\overline{y}_m^{[s]}$ is obtained by replacing all variables with a "bar" by the corresponding variables without a "bar", and vice versa. We assume that $h_{\mathcal{B}}(t) * s(t) = s(t)$.

Substituting (4) into (10), and using (8), we obtain the RP model of the received symbols:

$$y_m^{[s]} = x_m^{[s]} + w_m^{[s]} + \Delta x_m^{[s]}. \quad (11)$$

As in [20], the noise $w_m^{[s]}$ is independent and identically distributed (i.i.d.) complex Gaussian with variance N_{ASE}. Also as in [20], we neglect signal-noise mixing, and the nonlinear interference (NLI) becomes

$$\begin{aligned}
\Delta x_m^{[s]} = &\, j \sum_{s'} \sum_{\substack{n \\ k,k'}} S_{n,k,k'}^{[s,s']} x_{n+m}^{[s]} x_{k+m}^{[s']} x_{k'+m}^{[s'],*} \\
&+ j \sum_{s'} \sum_{\substack{n \\ k,k'}} \tilde{S}_{n,k,k'}^{[s,s']} x_{n+m}^{[s]} \overline{x}_{k+m}^{[s']} \overline{x}_{k'+m}^{[s'],*} \\
&+ j \sum_{s'} \sum_{c \neq 0} \sum_{\substack{n \\ k,k'}} C_{c;n,k,k'}^{[s,s']} x_{n+m}^{[s]} b_{c,k+m}^{[s']} b_{c,k'+m}^{[s'],*} \\
&+ j \sum_{s'} \sum_{c \neq 0} \sum_{\substack{n \\ k,k'}} \tilde{C}_{c;n,k,k'}^{[s,s']} x_{n+m}^{[s]} \overline{b}_{c,k+m}^{[s']} \overline{b}_{k'+m}^{[s'],*} \\
&+ j \sum_{r \neq s} \sum_{c \neq 0} \sum_{\substack{n \\ k,k'}} D_{c;n,k,k'}^{[s,r]} x_{n+m}^{[r]} b_{c,k+m}^{[s]} b_{c,k'+m}^{[r],*}. \\
&+ j \sum_{s'} \sum_{c \neq 0} \sum_{\substack{n \\ k,k'}} \tilde{D}_{c;n,k,k'}^{[s,s']} \overline{x}_{n+m}^{[s']} b_{c,k+m}^{[s]} \overline{b}_{c,k'+m}^{[s'],*}. \quad (12)
\end{aligned}$$

The coefficients in (12) can be written in terms of

$$\begin{aligned}
A_{n,k,k'}^{[s,s']}(t_1,t_2,t_3) = \gamma f_{s,s'} \int_0^{\mathcal{L}} \mathrm{d}z\, g_{s'}(z) \int_{-\infty}^{\infty} \mathrm{d}t\, s^*(z,t) \\
s(z, t - nT - t_1) s(z, t - kT - t_2) s^*(t - k'T - t_3). \quad (13)
\end{aligned}$$

We choose $\tau_0^{[s]} = 0$. For $r \neq s$, we have

$$S_{n,k,k'}^{[s,s']} = A_{n,k,k'}^{[s,s']}(0, \tau_0^{[s']}, \tau_0^{[s']}) \quad (14)$$

$$\tilde{S}_{n,k,k'}^{[s,s']} = A_{n,k,k'}^{[s,s']}(0, \overline{\tau}_0^{[s']}, \overline{\tau}_0^{[s']}) \quad (15)$$

$$C_{c;n,k,k'}^{[s,s]} = 2A_{n,k,k'}^{[s,s]}(0, \tau_c^{[s]} - \beta_2^{[s]}\Omega_c z, \tau_c^{[s]} - \beta_2^{[s]}\Omega_c z) \quad (16)$$

$$C_{c;n,k,k'}^{[s,r]} = A_{n,k,k'}^{[s,r]}(0, \tau_c^{[r]} - \beta_2^{[r]}\Omega_c z, \tau_c^{[r]} - \beta_2^{[r]}\Omega_c z) \quad (17)$$

$$\tilde{C}_{c;n,k,k'}^{[s,s']} = A_{n,k,k'}^{[s,s']}(0, \overline{\tau}_c^{[s']} - \beta_2^{[s']}\Omega_c z, \overline{\tau}_c^{[s']} - \beta_2^{[s']}\Omega_c z) \quad (18)$$

$$D_{c;n,k,k'}^{[s,r]} = A_{n,k,k'}^{[s,r]}(\tau_0^{[r]}, \tau_c^{[s]} - \beta_2^{[s]}\Omega_c z, \tau_c^{[r]} - \beta_2^{[r]}\Omega_c z) \quad (19)$$

$$\tilde{D}_{c;n,k,k'}^{[s,s']} = A_{n,k,k'}^{[s,s']}(\overline{\tau}_0^{[s']}, \tau_c^{[s]} - \beta_2^{[s]}\Omega_c z, \overline{\tau}_c^{[s']} - \beta_2^{[s']}\Omega_c z). \quad (20)$$

Using single-polarization DBP on the COI removes the terms with $S_{n,k,k'}^{[s,s]}$ from (12). Using dual-polarization DBP on the COI removes the terms with $S_{n,k,k'}^{[s,s]}$ or $\tilde{S}_{n,k,k'}^{[s,s]}$. Using multi-mode DBP removes all terms with $S_{n,k,k'}^{[s,s']}$ or $\tilde{S}_{n,k,k'}^{[s,s']}$.

Copyright (c) 2021 IEEE. Personal use is permitted. For any other purposes, permission must be obtained from the IEEE by emailing pubs-permissions@ieee.org.

IV. SDM-CRAN Model

As in [20], we gather all terms from (12) that depend on the current symbols. Assuming multi-mode DBP, we write

$$\begin{pmatrix} \Delta x_m^{[1]} \\ \overline{\Delta x}_m^{[1]} \\ \vdots \\ \Delta x_m^{[S]} \\ \overline{\Delta x}_m^{[S]} \end{pmatrix} = j\mathbf{J}_m \begin{pmatrix} x_m^{[1]} \\ \overline{x}_m^{[1]} \\ \vdots \\ x_m^{[S]} \\ \overline{x}_m^{[S]} \end{pmatrix} + \begin{pmatrix} v_m^{[1]} \\ \overline{v}_m^{[1]} \\ \vdots \\ v_m^{[S]} \\ \overline{v}_m^{[S]} \end{pmatrix} \tag{21}$$

where $\mathbf{J}_m$ is defined block-wise as

$$\mathbf{J}_m = \begin{pmatrix} \mathbf{D}_m^{[1,1]} & \mathbf{B}_m^{[1,2]} & \cdots & \mathbf{B}_m^{[1,S]} \\ \mathbf{B}_m^{[2,1]} & \mathbf{D}_m^{[2,2]} & \ddots & \mathbf{B}_m^{[2,S]} \\ \vdots & \ddots & \ddots & \vdots \\ \mathbf{B}_m^{[S,1]} & \mathbf{B}_m^{[S,2]} & \cdots & \mathbf{D}_m^{[S,S]} \end{pmatrix}. \tag{22}$$

The diagonal blocks (of size 2×2) are

$$\mathbf{D}_m^{[s,s]} = \begin{pmatrix} \theta_m^{[s]} & \psi_m^{[s,s]} \\ \overline{\psi}_m^{[s,s]} & \overline{\theta}_m^{[s]} \end{pmatrix} \tag{23}$$

and the off-diagonal blocks are

$$\mathbf{B}_m^{[s,r]} = \begin{pmatrix} \xi_m^{[s,r]} & \psi_m^{[s,r]} \\ \overline{\psi}_m^{[s,r]} & \overline{\xi}_m^{[s,r]} \end{pmatrix} \tag{24}$$

where, for $r \neq s$, we have

$$\theta_m^{[s]} = \sum_{s'} \sum_{c \neq 0} \sum_{k,k'} C_{c;0,k,k'}^{[s,s']} b_{c,k+m}^{[s']} b_{c,k'+m}^{[s'],*} + \sum_{s'} \sum_{c \neq 0} \sum_{k,k'} \tilde{C}_{c;0,k,k'}^{[s,s']} \overline{b}_{c,k+m}^{[s']} \overline{b}_{k'+m}^{[s'],*} \tag{25}$$

$$\psi_m^{[s,s']} = \sum_{c \neq 0} \sum_{k,k'} \tilde{D}_{c;0,k,k'}^{[s,s']} b_{c,k+m}^{[s]} \overline{b}_{c,k'+m}^{[s'],*}. \tag{26}$$

$$\xi_m^{[s,r]} = \sum_{c \neq 0} \sum_{k,k'} D_{c;0,k,k'}^{[s,r]} b_{c,k+m}^{[s]} b_{c,k'+m}^{[r],*} \tag{27}$$

and $\overline{\theta}_m^{[s]}$, $\overline{\psi}_m^{[s,s']}$, and $\overline{\xi}_m^{[s,r]}$ are obtained by swapping $b_{c,\ell}^{[i]}$ with $\overline{b}_{c,\ell}^{[i]}$ in (25)-(27), swapping $\tau_c^{[i]}$ with $\overline{\tau}_c^{[i]}$ in (14)-(20), and shifting all delays such that $\overline{\tau}_0^{[s]} = 0$. The residual NLI terms $v_m^{[s]}$ and $\overline{v}_m^{[s]}$ are given by (12) without the two first lines (in the DBP case) and without the summands with $n = 0$.

We choose all pulses of the same frequency channel to be synchronized, i.e., we set $\tau_c^{[s]} = \overline{\tau}_c^{[s]} := \tau_c$ for all s and c.[2] We thus have $\tilde{D}_{c;0,k,k'}^{[s,s']} = \tilde{D}_{c;0,k',k}^{[s',s],*}$, $D_{c;0,k,k'}^{[s,s']} = D_{c;0,k',k}^{[s',s],*}$, and

$$\psi_m^{[s,s']} = \overline{\psi}_m^{[s',s],*}, \quad \xi_m^{[s,r]} = \xi_m^{[r,s],*}, \quad \overline{\xi}_m^{[s,r]} = \overline{\xi}_m^{[r,s],*}. \tag{28}$$

Since the $\theta_m^{[s]}$ and $\overline{\theta}_m^{[s]}$ are real [20], the matrix $\mathbf{J}_m$ is Hermitian. Using (25)-(27), it follows that all the diagonal terms $\Theta_m^{[s]}$ and $\overline{\Theta}_m^{[s]}$ are correlated and all other crosscorrelations are 0.

[2]For multi-carrier transmission, the $2S$ pulses of each subcarrier are synchronized but the pulses of different subcarriers are not.

A. Mode Rotation Approximation

As in [20], we apply an LP-like approximation

$$\mathbf{I} + j\mathbf{J}_m \approx \exp\left(j\mathbf{J}_m\right). \tag{29}$$

Using (21) and (11), we write the SDM-CRAN model as

$$\mathbf{y}_m = \exp\left(j\mathbf{J}_m\right) \mathbf{x}_m + \mathbf{v}_m + \mathbf{w}_m \tag{30}$$

where $\mathbf{y}_m = (y_m^{[1]}, \overline{y}_m^{[1]}, \cdots, y_m^{[S]}, \overline{y}_m^{[S]})^T$, and $\mathbf{x}_m$, $\mathbf{v}_m$, and $\mathbf{w}_m$ are defined similarly. The matrix $\exp\left(j\mathbf{J}_m\right) \in \mathbb{C}^{2S \times 2S}$ is unitary. The components of the residual NLI $\mathbf{v}_m$ are uncorrelated and have memory in the time parameter m, see [20]. The statistics of the entries of $\mathbf{J}_m$ can be derived as in [20]. We state results for strong coupling next.

B. Statistics of $\mathbf{J}_m$ for Strong Coupling

Strong coupling has $f_{s,s'} = \kappa$, $\beta_2^{[s]} = \beta_2$ and $g_s(z) = g(z)$. Furthermore, all the coefficients of the same frequency channel c, except for $C_{c;n,k,k'}^{[s,s]}$, are equal and independent of s, s', and r. We call these coefficients $X_{c;n,k,k'}$:

$$\begin{aligned} X_{c;n,k,k'} &:= \frac{C_{c;n,k,k'}^{[s,s]}}{2} = C_{c;n,k,k'}^{[s,r]} = \tilde{C}_{c;n,k,k'}^{[s,s']} \\ &= D_{c;n,k,k'}^{[s,r]} = \tilde{D}_{c;n,k,k'}^{[s,s']} \end{aligned} \tag{31}$$

for all s, s' and all $r \neq s$. The means of the entries $J_{i,k}[m]$ of the matrix $\mathbf{J}_m$ in (30) are

$$\langle J_{i,i}[m] \rangle = (1 + 2S) \sum_{c \neq 0} E_c \sum_k X_{c;0,k,k'} \tag{32}$$

$$\langle J_{i,k}[m] \rangle = 0, \quad k \neq i. \tag{33}$$

The auto- and crosscovariance functions of the $J_{i,k}[m]$ can be written in terms of the following two functions:

$$\begin{aligned} r[\ell] = &\sum_{c \neq 0} (Q_c - E_c^2) \sum_k X_{c;0,k,k} X_{c;0,k-\ell,k-\ell} \\ &+ \sum_{c \neq 0} E_c^2 \sum_{k \neq k'} X_{c;0,k,k'} X_{c;0,k-\ell,k'-\ell}^* \end{aligned} \tag{34}$$

$$s[\ell] = \sum_{c \neq 0} E_c^2 \sum_{k,k'} X_{c;0,k,k'} X_{c;0,k-\ell,k'-\ell}^*. \tag{35}$$

If one defines

$$r_{iki'k'}[\ell] = \left\langle J_{i,k}[m] J_{i',k'}^*[m+\ell] \right\rangle - \langle J_{i,k}[m] \rangle \left\langle J_{i',k'}^*[m+\ell] \right\rangle \tag{36}$$

then the autocovariance functions are

$$r_{iiii}[\ell] = (3 + 2S) r[\ell] \tag{37}$$

$$r_{ikik}[\ell] = s[\ell], \quad k \neq i; \tag{38}$$

the crosscovariance function of two diagonal elements is

$$r_{iikk}[\ell] = (2 + 2S) r[\ell], \quad k \neq i; \tag{39}$$

and the other crosscorrelation functions are 0:

$$r_{iii'k'}[\ell] = 0, \quad i' \neq k' \tag{40}$$

$$r_{iki'k'} = 0, \quad (i,k) \neq (i',k') \text{ and } (i,k) \neq (k',i') \tag{41}$$

where we recall that $\mathbf{J}_m$ is Hermitian. If the inputs $B_{c,k}^{[s]}$ and $\overline{B}_{c,k}^{[s]}$ are CSCG, then we have $r[\ell] = s[\ell]$. In the limit of large

Copyright (c) 2021 IEEE. Personal use is permitted. For any other purposes, permission must be obtained from the IEEE by emailing pubs-permissions@ieee.org.

accumulated dispersion, the approximations introduced in [23] apply (see [19], [20]):

$$\langle J_{i,i}[m]\rangle \approx (1+2S)\gamma\kappa\frac{\mathcal{L}}{T}\sum_{c\neq 0}E_c \tag{42}$$

$$r[\ell] \approx \frac{\gamma^2\kappa^2\mathcal{L}}{T}\sum_{c\neq 0}\frac{Q_c-E_c^2}{|\beta_2\Omega_c|}\left[1-\frac{|\ell|T}{|\beta_2\Omega_c|\,\mathcal{L}}\right]^+ \tag{43}$$

$$s[\ell] \approx \frac{\gamma^2\kappa^2\mathcal{L}}{T}\sum_{c\neq 0}\frac{E_c^2}{|\beta_2\Omega_c|}\left[1-\frac{|\ell|T}{|\beta_2\Omega_c|\,\mathcal{L}}\right]^+ \tag{44}$$

where one assumes that the contributions of the summands with $X_{c;0,k,k}$ in (34) and (35) dominate, see [20, Fig. 2]. For example, in a 2-pol system ($S=1$), the ACF $r_\Theta[\ell]$ of the diagonal elements of $\mathbf{J}_m$ is $5r[\ell]$ (see (37)), with $r[\ell]$ approximately given by (43). This matches [20, Eq. (75)].

V. Simplified SDM-CRAN Model

In the following, the receiver removes the means $\left\langle\Theta_m^{[s]}\right\rangle \equiv \langle J_{2s-1,2s-1}[m]\rangle$ and $\left\langle\overline{\Theta}_m^{[s]}\right\rangle \equiv \langle J_{2s,2s}[m]\rangle$ of the phase noise, and we abuse notation and write $J_{i,i}[m]$ for the resulting zero-mean variables. Based on the statistical analysis of Section IV-B, we model the entries of the matrix $\mathbf{J}_m$ in (30) as

$$j_{i,i}[m] = 2\phi_i[m] + \sum_{i'\neq i}\phi_{i'}[m] \tag{45}$$

$$j_{k,i}[m] = j_{i,k}^*[m] \tag{46}$$

where the $\Phi_i[m]$, $i=1,\ldots,2S$, are independent, real, Gaussian, memory-μ Markov processes generated using the procedure in [20, Section IV.B] with autocovariance function $r[\ell]$ in (34) for $\ell\in\{-\mu,\ldots,\mu\}$. The $J_{i,k}[m]$ for $i<k$ are independent CSCG memory-μ Markov processes generated using the same procedure with autocovariance function $s[\ell]$ in (35) for $\ell\in\{-\mu,\ldots,\mu\}$. The number of hidden independent *real* Markov processes in $\mathbf{J}_m$ is thus $4S^2$, of which $2S$ are the $\Phi_i[m]$.

As in [19], [20], we combine the ASE noise and the residual NLI noise into one additive noise term $\mathbf{z}_m=\mathbf{v}_m+\mathbf{w}_m$. The simplified (mismatched) SDM-CRAN model is

$$\mathbf{y}_m = \exp(j\mathbf{J}_m)\,\mathbf{x}_m + \mathbf{z}_m. \tag{47}$$

We model the entries $Z_i[m]$ of $\mathbf{z}_m$ as independent CSCG processes with real ACFs

$$r_{Z_i}[\ell] := \langle Z_i[m]Z_i^*[m+\ell]\rangle = N_{\text{ASE}}\delta[\ell] + \langle V_i[m]V_i^*[m+\ell]\rangle \tag{48}$$

where $v_i[m]$ is the i-th entry of $\mathbf{v}_m$. The ACF $r_{Z_i}[\ell]$ has short memory and a similar shape as [19, Fig. 3].

VI. Numerical Results

A. Estimating Model Parameters

We use a training set to estimate the parameters of the model (47). Since the matrix $\exp(j\mathbf{J}_m)$ in (47) is unitary, if we use i.i.d. Gaussian inputs $\mathbf{x}_m$ and neglect the small correlations in $\mathbf{Z}_m$ then the distribution of $\|\mathbf{Y}_m\|^2$ given $\|\mathbf{X}_m\|$ is noncentral chi-squared with $4S$ degrees of freedom, and independent for each m. We thus estimate the noise variance $\sigma_Z^2 = r_{Z_i}[0]$ as

$$\hat{\sigma}_Z^2 = \arg\max_{\sigma^2}\sum_m \log\left[\frac{e^{-\frac{\|\mathbf{y}_m\|^2+\|\mathbf{x}_m\|^2}{\sigma^2}}}{\sigma^2}\frac{\|\mathbf{y}_m\|^{2S-1}}{\|\mathbf{x}_m\|^{2S-1}}I_{2S-1}\left(\frac{2\|\mathbf{y}_m\|\|\mathbf{x}_m\|}{\sigma^2}\right)\right]. \tag{49}$$

We estimate the mean phase noise $\langle J_{i,i}[m]\rangle$ as in [20]. For the matrix $\mathbf{J}_m$, we assume that all $\Phi_i[m]$ (see (45)) have the same ACF $\sigma_\Phi^2 r[\ell]$, and that all $J_{k,i}[m]$ for $k<i$ have the same ACF $\sigma_J^2 s[\ell]$, with $r[\ell]$ and $s[\ell]$ given by (43) and (44). We minimize the mismatched conditional entropy $h_q(\mathbf{Y}|\mathbf{X})$ (obtained using particle filtering [20]) over σ_Φ^2 and σ_J^2. We use the same symmetric, real, three-tap, unit-energy whitening filter on all modes, and minimize $h_q(\mathbf{Y}|\mathbf{X})$ over its free parameter.

TABLE I
System parameters

Parameter	Symbol	Value
Dispersion coefficient	β_2	-21.7 ps^2/km
Nonlinear coefficient	γ	1.27 W^{-1}km^{-1}
RX noise spectral density	N_{ASE}	$5.902\cdot 10^{-18}$ W/Hz
Number of spatial modes	S	2
WDM channel indexes	$c_{\min}, c_{\max}$	$-2, 2$
Transmitted pulse shape	$s(t)$	sinc
Channel bandwidth	$\mathcal{B}$	50 GHz
Channel spacing	$\Omega^{(1)}/(2\pi)$	50 GHz

B. Achievable Rates

We simulated the strong coupling system (3) with $S=2$ spatial modes and 5 WDM channels by using the split-step Fourier method. The system has IDA and the parameters in Table I. As in [20], we compare single- and multi-carrier systems, where the latter system has four subcarriers (4SC) of bandwidth 12.5 GHz each. All subcarriers have the same power, i.e., there is no frequency-dependent power allocation as in [19], [20]. The input symbols have a Gaussian density. The channel delays τ_c are chosen randomly between $-T/2$ and $T/2$. The receiver applies a 50-GHz band-pass filter to isolate the COI, followed by joint DBP on all COI spatial modes and subcarriers, and then matched filtering and sampling. A training set of 24 sequences of 4092 symbols (20 sequences of 4×1023 symbols in the 4SC system) is used to estimate the SDM-CRAN model parameters.

We apply particle filtering on a test set of 120 sequences (100 sequences for 4SC) to compute achievable rates as described in [20, Sec. VI]. The mismatched output distribution is Gaussian [20, Eq. (91)]. The results are plotted in Fig. 1 that compares four receiver algorithms with successively more complex processing:

- separate processing of each of the $2S$ (complex-alphabet) channels using a memoryless mismatched model with i.i.d. phase-and-additive noise, see [19, Sec. VIII.A];
- separate 1-pol CPAN (1pCPAN) processing of each of the $2S$ channels with $2S$ particle filters, see [19];

Copyright (c) 2021 IEEE. Personal use is permitted. For any other purposes, permission must be obtained from the IEEE by emailing pubs-permissions@ieee.org.

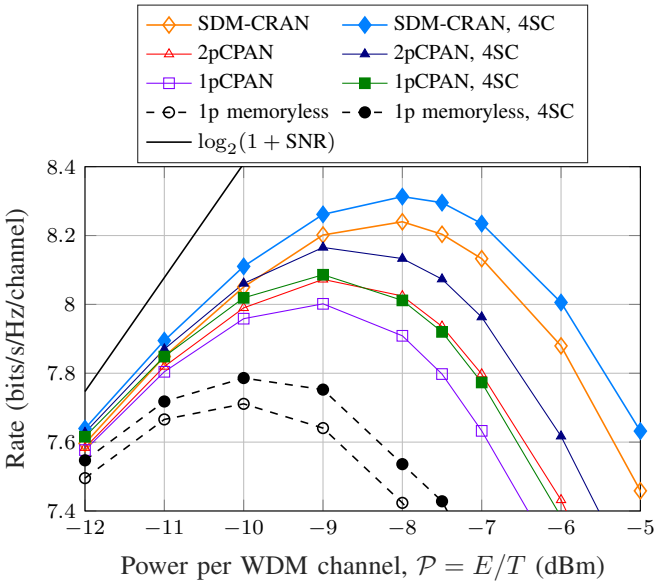

Fig. 1. Achievable rates for a 1000-km SDM link with $S = 2$ spatial modes, 5 WDM channels, strong coupling, and the parameters in Table I. SNR $= P/(N_{\text{ASE}}\mathcal{B})$

- separate 2-pol CPAN (2pCPAN) processing of the S spatial modes with S particle filters, see [20];
- joint CRAN processing of all $2S$ channels with one particle filter that uses the mismatched model (45)-(48).

With respect to memoryless processing, the 1pCPAN model gains 0.29 bits/s/Hz/channel, the 2pCPAN model gains a further 0.07 bits/s/Hz/channel, and the SDM-CRAN model gains another 0.17 bits/s/Hz/channel. 4SC gains between 0.07 and 0.1 bits/s/Hz/channel with respect to single-carrier transmission. The rate gain from the peak of the lowermost curve to the peak of the uppermost curve is approximately 0.6 bits/s/Hz/channel. The rate gain from "Memoryless" to "SDM-CRAN" for either single- or multi-carrier transmission is 0.5 bits/s/Hz/channel. For 4SC, the power gain from the rate peak with memoryless processing to the SDM-CRAN curve at the same rate (7.79 bits/s/Hz/channel) is 1.4 dB.

VII. Conclusions

We extended the analysis of the CPAN model [19], [20] to SDM for weak and strong coupling. The SDM-CRAN model and a multi-carrier scheme were applied to strong coupling to obtain achievable rates for a $S = 2$ spatial mode system. The rates are 0.6 bits/s/Hz/channel larger than the rates for a single-carrier system with separate and memoryless processing per complex-alphabet channel.

We remark that computational complexity limits the numerical calculations to a small number S of spatial modes. An important direction for future work is speeding up the calculations and designing simplified receivers that exploit the correlations predicted by the SDM-CRAN model in practical multi-mode systems. An interesting theory question is to extend the LP analyses of [14]–[16] to SDM.

References

[1] D. J. Richardson, J. M. Fini, and L. E. Nelson, "Space-division multiplexing in optical fibres," *Nature Photonics*, vol. 7, pp. 354 – 362, Apr. 2013.

[2] D. Soma *et al.*, "10.16 peta-bit/s dense SDM/WDM transmission over low-DMD 6-mode 19-core fibre across C+L band," in *Eur. Conf. Optical Commun. (ECOC)*, 2017.

[3] R. Ryf *et al.*, "Transmission over randomly-coupled 4-core fiber in field-deployed multi-core fiber cable," in *Eur. Conf. Optical Commun. (ECOC)*, 2020.

[4] R. S. Luís *et al.*, "Experimental demonstration of a petabit per second SDM network node," *J. Lightw. Technol.*, vol. 38, no. 11, pp. 2886–2896, Jun. 2020.

[5] G. Kramer, M. I. Yousefi, and F. R. Kschischang, "Upper bound on the capacity of a cascade of nonlinear and noisy channels," in *IEEE Inf. Theory Workshop*, Apr. 2015.

[6] M. I. Yousefi, G. Kramer, and F. R. Kschischang, "Upper bound on the capacity of the nonlinear Schrödinger channel," in *IEEE Can. Workshop Inf. Theory*, Jul. 2015, pp. 22–26.

[7] R. J. Essiambre, G. Kramer, P. J. Winzer, G. J. Foschini, and B. Goebel, "Capacity limits of optical fiber networks," *J. Lightw. Technol.*, vol. 28, no. 4, pp. 662–701, Feb. 2010.

[8] P. Poggiolini, G. Bosco, A. Carena, V. Curri, Y. Jiang, and F. Forghieri, "The GN-model of fiber non-linear propagation and its applications," *J. Lightw. Technol.*, vol. 32, no. 4, pp. 694–721, Feb. 2014.

[9] A. Carena, G. Bosco, V. Curri, Y. Jiang, P. Poggiolini, and F. Forghieri, "EGN model of non-linear fiber propagation," *Opt. Express*, vol. 22, no. 13, pp. 16 335–16 362, Jun. 2014.

[10] A. Mecozzi, C. B. Clausen, and M. Shtaif, "Analysis of intrachannel nonlinear effects in highly dispersed optical pulse transmission," *IEEE Photon. Technol. Lett.*, vol. 12, no. 4, pp. 392–394, Apr. 2000.

[11] ——, "System impact of intra-channel nonlinear effects in highly dispersed optical pulse transmission," *IEEE Photon. Technol. Lett.*, vol. 12, no. 12, pp. 1633–1635, Dec. 2000.

[12] A. Vannucci, P. Serena, and A. Bononi, "The RP method: a new tool for the iterative solution of the nonlinear Schrödinger equation," *J. Lightw. Technol.*, vol. 20, no. 7, pp. 1102–1112, Jul. 2002.

[13] A. Mecozzi and R. Essiambre, "Nonlinear Shannon limit in pseudolinear coherent systems," *J. Lightw. Technol.*, vol. 30, no. 12, pp. 2011–2024, Jun. 2012.

[14] E. Ciaramella and E. Forestieri, "Analytical approximation of nonlinear distortions," *IEEE Phot. Technol. Lett.*, vol. 17, no. 1, pp. 91–93, Jan. 2005.

[15] E. Forestieri and M. Secondini, "Solving the nonlinear Schrödinger equation," in *Optical Communication Theory and Techniques*, E. Forestieri, Ed. Boston, MA: Springer, 2005, pp. 3–11.

[16] M. Secondini, E. Forestieri, and C. R. Menyuk, "A combined regular-logarithmic perturbation method for signal-noise interaction in amplified optical systems," *J. Lightw. Technol.*, vol. 27, no. 16, pp. 3358–3369, Aug. 2009.

[17] M. Secondini, E. Forestieri, and G. Prati, "Achievable information rate in nonlinear WDM fiber-optic systems with arbitrary modulation formats and dispersion maps," *J. Lightw. Technol.*, vol. 31, no. 23, pp. 3839–3852, Dec. 2013.

[18] M. Secondini, E. Agrell, E. Forestieri, D. Marsella, and M. R. Camara, "Nonlinearity mitigation in WDM systems: Models, strategies, and achievable rates," *J. Lightw. Technol.*, vol. 37, no. 10, pp. 2270–2283, May 2019.

[19] F. J. García-Gómez and G. Kramer, "Mismatched models to lower bound the capacity of optical fiber channels," *J. Lightw. Technol.*, vol. 38, no. 24, pp. 6779–6787, Dec. 2020.

[20] F. J. García-Gómez and G. Kramer, "Mismatched models to lower bound the capacity of dual-polarization optical fiber channels," *J. Lightw. Technol.*, vol. 39, no. 11, pp. 3390–3399, Jun. 2021.

[21] S. Mumtaz, R.-J. Essiambre, and G. P. Agrawal, "Nonlinear propagation in multimode and multicore fibers: Generalization of the manakov equations," *J. Lightw. Technol.*, vol. 31, no. 3, pp. 398–406, 2013.

[22] A. Mecozzi, C. Antonelli, and M. Shtaif, "Coupled Manakov equations in multimode fibers with strongly coupled groups of modes," *Opt. Express*, vol. 20, no. 21, pp. 23 436–23 441, Oct. 2012.

[23] R. Dar, M. Feder, A. Mecozzi, and M. Shtaif, "Properties of nonlinear noise in long, dispersion-uncompensated fiber links," *Opt. Express*, vol. 21, no. 22, pp. 25 685–25 699, Nov. 2013.

Copyright (c) 2021 IEEE. Personal use is permitted. For any other purposes, permission must be obtained from the IEEE by emailing pubs-permissions@ieee.org.